Cholesterol deficiency in a mouse model of Smith-Lemli-Opitz syndrome reveals increased mast cell responsiveness

Martina Kovarova,[1] Christopher A. Wassif,[2] Sandra Odom,[1] Katherine Liao,[1] Forbes D. Porter,[2] and Juan Rivera[1]

[1]Molecular Inflammation Section, Molecular Immunology and Inflammation Branch, National Institute of Arthritis and Musculoskeletal and Skin Diseases, and [2]Unit on Molecular Dysmorphology, Heritable Disorders Branch, National Institute of Child Health and Human Development, National Institutes of Health (NIH), Department of Health and Human Services, Bethesda, MD 20892

Mutation of the 3β-hydroxysterol Δ^7-reductase gene (*Dhcr7*$^{-/-}$) results in Smith-Lemli-Opitz syndrome (SLOS). Patients, and genetically altered mice, are unable to produce cholesterol and accumulate 7-dehydrocholesterol (DHC) in serum and tissue. This causes multiple growth and developmental abnormalities as well as immune system anomalies including allergy. Because cholesterol is a key component of liquid-ordered membranes (lipid rafts) and these domains have been implicated in regulating mast cell activation, we examined whether mast cell responsiveness is altered in this model. Mast cells derived from *Dhcr7*$^{-/-}$ mice (DHCR KO) showed constitutive cytokine production and hyper-degranulation after stimulation of the high affinity IgE receptor (FcεRI). DHCR KO mast cells, but not wild-type mast cells, accumulated DHC in lipid rafts. DHC partially disrupted lipid raft stability and displaced Lyn kinase protein and activity from lipid rafts. This led to down-regulation of some Lyn-dependent signaling events but increased Fyn kinase activity and Akt phosphorylation. The Lyn-dependent phosphorylation of Csk-binding protein, which negatively regulates Fyn activity, was decreased. This phenotype reproduces some of the characteristics of Lyn-null mast cells, which also demonstrate hyper-degranulation. These findings provide the first evidence of lipid raft dysfunction in SLOS and may explain the observed association of allergy with SLOS.

CORRESPONDENCE
Juan Rivera:
juan_rivera@nih.gov

Abbreviations used: Ag, antigen; Cbp, Csk-binding protein; DHC, 7-dehydrocholesterol; GC, gas chromatography; LPDS, lipoprotein-deficient serum; MBCD, methyl-β-cyclodextrin; PI3K, phosphatidylinositol 3-OH kinase; PLCγ, phospholipase C-γ; SLOS, Smith-Lemli-Opitz syndrome.

Smith-Lemli-Opitz syndrome (SLOS) is an autosomal recessive genetic disease with an incidence of 1 in 50,000. It is characterized by mental retardation, microcephaly, syndactyly of the toes, and other dysmorphic features and problems related to abnormal growth and development. SLOS is caused by mutation of the 3β-hydroxysterol-Δ^7-reductase gene (*DHCR7*), which converts 7-dehydrocholesterol (DHC) to cholesterol (1–3). SLOS-affected individuals have increased plasma levels of DHC and abnormally low levels of cholesterol. Many of these patients experience formula and food intolerance. Because mast cells are central in allergy and cholesterol-enriched liquid-ordered domains (lipid rafts) play an important role in their activation (4, 5), it was of interest to study whether the loss of cholesterol altered mast cell sensitivity and activation. Mice carrying a null mutation of the 3 β-hydroxysterol-Δ^7-reductase gene (*Dhcr7*$^{-/-}$, referred to as DHCR KO throughout) were developed as a model for SLOS (6). These mice failed to produce cholesterol and accumulated DHC in serum and tissue. Due to a failure to nurse, newborn mice die shortly after birth. We were able, however, to cultivate mast cells from the liver progenitors of DHCR KO mice.

Cholesterol plays an important role in membrane organization (7, 8). The plasma membrane has specialized regions that are characterized by high concentrations of cholesterol and sphingolipids and spontaneously segregate and are insoluble in nonionic detergents (9). Antigen (Ag)-induced aggregation of FcεRI-bound IgE antibodies causes inclusion of this receptor in these specialized regions commonly referred to as lipid rafts. Lyn kinase is also concentrated in lipid rafts (4, 5) and weakly associates and phosphorylates FcεRI (10). Whether

The online version of this article contains supplemental material.

Vol. 203, No. 5, May 15, 2006 1161–1171 www.jem.org/cgi/doi/10.1084/jem.20051701

the recruitment of FcεRI into lipid rafts is necessary for its interaction with Lyn and for initiation of its phosphorylation, or whether lipid rafts serve to sustain and/or amplify the receptors' phosphorylation remains unresolved. The mouse SLOS model studied herein provided a system where depletion of cholesterol could be achieved as a consequence of gene deletion. Because cholesterol plays a crucial role in membrane domains with signal transduction potential (8), investigating the molecular consequences of cholesterol deficiency and DHC accumulation in mast cell function could yield new insights for understanding the pathophysiology underlying SLOS and disease treatment.

RESULTS

Mast cells deficient in 3-β-hydroxysterol-Δ^7-reductase accumulate DHC

Mast cell progenitors from both DHCR KO and WT mice were cultivated in medium with cholesterol. DHCR KO mast cells cultivated in medium containing 10% FBS proliferated and differentiated similarly to WT mast cells. No substantial differences were found in global tyrosine phosphorylation of proteins, intracellular calcium release, or in degranulation of DHCR KO mast cells cultivated under these conditions (Fig. 1 A and not depicted). Cholesterol levels were the same in DHCR KO and WT mast cells (Table I, 0 h), demonstrating that growth of these cells in medium containing cholesterol bypassed the defect of 3-β-hydroxysterol-Δ^7-reductase mutation.

To reveal the biosynthetic defect, mature DHCR KO or WT mast cells were cultured in medium supplemented with lipoprotein-deficient serum (LPDS). Cell viability, as determined by propidium iodide staining, and sterol content were measured up to 120 h after depletion. WT mast cells proliferated in medium without cholesterol for 120 h (Fig. S1, available at http://www.jem.org/cgi/content/full/jem.20051701/DC1) without a significant decrease in cell viability (Table I). Cholesterol content decreased within 48 to 72 h of depletion by ∼30% and subsequently increased to reach original levels by 120 h, demonstrating activation of cholesterol biosynthesis. Desmosterol, a precursor of cholesterol, was also detected in WT mast cells at 48 and 72 h but not at 0 h (Table I). Levels of desmosterol reached ∼20–30% of total sterol at 72 h. In contrast, DHCR KO cells preferentially accumulated DHC as the cholesterol content decreased (Table I), and DHC levels peaked at ∼30% of total sterols between 72 and 96 h of depletion. Total sterol content was relatively constant in WT cells but decreased slightly in DHCR KO cells. DHCR KO mast cells also proliferated poorly (Fig. S1) and cell viability decreased with time (Table I). When grown for 168 h in LPDS, cell viability was <70% (not depicted).

Subsequent experiments were performed with cells grown in LPDS for 72 h, as cell viability was normal and the ratio of DHC or desmosterol to total sterol was maximal (Table I). The numbers of apoptotic cells did not differ substantially between cholesterol-depleted and nondepleted

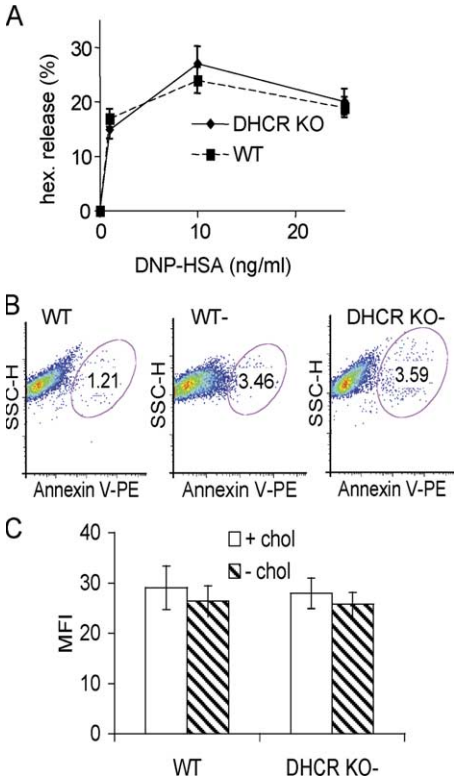

Figure 1. Characterization of mast cell FcεRI expression, survival, and function from DHCR KO mice. (A) Mast cells derived from the liver progenitors of WT or DHCR KO mice were cultivated in medium with normal FBS, IL-3, and stem cell factor for 4 wk. Cells were sensitized with DNP-specific IgE for 60 min and activated by exposure to the indicated concentration of DNP-HSA for 20 min. Hexosaminidase release is expressed as a percentage of total cellular hexosaminidase. Data is mean ± SEM from four individual experiments. (B) Apoptotic cells were stained with PE-labeled annexin V in WT nondepleted or WT and DHCR KO cells depleted in cholesterol-free medium for 72 h and analyzed by FACS. One representative of >12 individual cultures is shown. (C) WT or DHCR KO mast cells were cultivated in normal or cholesterol-free medium for 72 h and loaded with IgE, washed, and followed by FITC-labeled anti-IgE antibody. Level of FcεRI expression was determined as the mean fluorescence intensity (MFI) in FITC anti-IgE–stained cells compared with isotype control. Data is mean ± SD from three individual experiments.

cells and did not exceed 7% of total cells (Fig. 1 B). FcεRI expression before or after cholesterol depletion was similar among WT and DHCR KO mast cells (Fig. 1 C). Thus, for further experiments, we compared cholesterol-depleted DHCR KO mast cells with cholesterol-depleted or nondepleted WT mast cells.

Loss of cholesterol and accumulation of DHC in mast cells result in FcεRI-dependent hyperresponsiveness

FcεRI-dependent degranulation of cholesterol-depleted DHCR KO cells showed a 2.8-fold increase ($P < 0.006$, $n = 15$) over nondepleted WT mast cells in release of the granule marker hexosaminidase (Fig. 2, A and B). Cholesterol-depleted WT cells also showed a twofold increase ($P < 0.02$,

Table I. Effect of cholesterol depletion on mast cell sterol content and viability

Time of cholesterol depletion (h)	DHCR KO			WT		
	Cholesterol (μg/mg of protein)	DHC (μg/mg of protein)	Viability (%)	Cholesterol (μg/mg of protein)	Desmosterol (μg/mg of protein)	Viability (%)
0	3.6 ± 0.3 (10)	0.3 ± 0.1 (10)	96.4 ± 0.3 (6)	3.9 ± 0.3 (10)	nd	96.9 ± 0.3 (6)
48	2.6 ± 0.2 (3)	0.5 ± 0.1 (3)	95.1 ± 0.1 (3)	2.7 ± 0.2 (3)	0.6 ± 0.3 (3)	96.8 ± 0.2 (3)
72	2.2 ± 0.3 (10)	0.9 ± 0.4 (10)	93.6 ± 0.3 (6)	2.9 ± 0.3 (10)	1.3 ± 0.5 (3)	96.9 ± 0.1 (6)
96	1.9 ± 0.1 (3)	1.1 ± 0.2 (3)	89.7 ± 0.6 (3)	3.3 ± 0.1 (3)	nd	95.2 ± 0.3 (3)
120	2.4 ± 0.2 (4)	1.1 ± 0.1 (4)	89.3 ± 0.8 (3)	3.4 ± 0.1 (5)	nd	95.0 ± 0.2 (3)

Cells were depleted of cholesterol by incubation for the indicated times in medium containing LPDS. Cell viability was monitored by trypan blue exclusion and propidium iodide staining. Content of cholesterol, DHC, and desmosterol was determined by GC/mass spectrometry analysis of extracted sterols. DHC was also measured in cholesterol-depleted WT cells but was nondetectable (sensitivity of assay is pg/mg of protein, $n = 5$). Total sterols did not differ significantly among genotypes before or after cholesterol depletion (0 vs. 72 h). Data shown are the mean ± SEM for replicate numbers as indicated in parenthesis. nd, not detected.

$n = 15$) relative to nondepleted WT cells. Total amounts of cellular hexosaminidase did not differ.

This suggested that the augmentation of degranulation resulted from cholesterol depletion and/or accumulation of DHC. To test this, cholesterol-depleted WT and DHCR KO mast cells were reconstituted with cholesterol by cultivation in medium containing 30% FBS for 30 min. The concentration of cholesterol in the repleted WT and DHCR KO cells increased to levels equivalent to nondepleted cells as determined by gas chromatography (GC)/mass spectrometry (Table I and not depicted). Cholesterol repletion of WT mast cells reduced degranulation to the level of nondepleted WT mast cells (Fig. 2 C). In contrast, cholesterol-repleted DHCR KO mast cells still had enhanced degranulation relative to cholesterol-repleted or nondepleted WT mast cells. This suggested that the accumulation of DHC in DHCR KO mast cells, but not the accumulation of desmosterol in WT cells, contributed to the maintenance of enhanced degranulation. The concentration of DHC ($R^2 = 0.6094$, $P < 0.03$), but not the concentration of cholesterol ($R^2 = 0.0246$, $P > 0.70$) or of total sterol ($R^2 = 0.0114$, $P > 0.80$; not depicted), correlated with increased degranulation (Fig. 2, D and E) in DHCR KO mast cells. In contrast, cholesterol correlated ($R^2 = 0.740$, $P < 0.01$) with degranulation of cholesterol-depleted WT (Fig. 2 F). Thus, control of WT mast cell degranulation appeared to be dependent on cholesterol, whereas DHC caused an irreversible enhancement of degranulation. The observed effect of cholesterol or DHC on mast cell degranulation was upstream of the exocytotic machinery because PMA and calcium ionophore A23187 (a stimulus that bypasses early signaling events) led to similar degranulation from cholesterol-depleted or nondepleted cells (Fig. 2 G). Granule membrane integrity (as determined with toluidine blue) did not differ as a consequence of cholesterol depletion or gene alteration (not depicted).

As shown in Fig. 2 H, constitutive secretion of both IL-6 and TNF was observed after cholesterol depletion. Constitutive TNF secretion by DHCR KO mast cells was considerable (105 ± 6.3 pg/ml/10^6 cells), reaching ~40% of the response of stimulated WT control cells (246 ± 17.1 pg/ml/10^6 cells). FcεRI stimulation did not substantially augment this secretion. IL-6 secretion was also constitutive after cholesterol depletion of DHCR KO (223 ± 9 pg/ml/10^6 cells), reaching approximately one third the level of stimulated control WT mast cells (643 ± 37 pg/ml/10^6 cells). For cholesterol-depleted WT mast cells, IL-6 secretion was also constitutive and significant ($P < 0.05$, $n = 4$) relative to nondepleted cells. For TNF, a consistent but not significant ($P < 0.09$) increase was observed. Thus, the higher constitutive secretion of IL-6 and TNF from cholesterol-depleted DHCR KO cells suggested that the accumulation of DHC played an important role in the enhanced cytokine response.

Accumulation of DHC in lipid rafts partially decreases their stability

To gain an understanding of the role of DHC in cell membranes, we isolated lipid rafts from WT and DHCR KO mast cells. Both cholesterol and DHC were considerably partitioned to these domains (Fig. 3 A). The lipid raft fractions (1–4) contained 60 ± 2% of the total cholesterol, and the relative distribution of cholesterol did not change during depletion (Fig. 3 A), although the absolute amount of cholesterol decreased in WT cells at 72 h (Table I). For DHCR KO mast cells, the DHC content in lipid rafts was 84 ± 14% of the total DHC in these cells, and the amount of total sterols in lipid rafts was slightly increased. We subsequently tested whether the presence of DHC in lipid rafts influenced their stability. The ease of solubility in Triton X-100 was used as a measure of lipid raft stability (11). Multilamellar lipid vesicles were prepared from cellular lipids, and solubility was measured in 0.075 and 0.1% Triton X-100. As shown in Fig. 3 B, multilamellar vesicles from cholesterol-depleted DHCR KO mast cells had significantly higher solubility compared with vesicles from cholesterol-depleted or nondepleted WT cells. The relative effectiveness of methyl-β-cyclodextrin (MBCD) to remove cholesterol from the plasma membrane is also indicative of cholesterol packing and lipid raft stability (12). Incubation of cells with 5mM MBCD demonstrated more efficient extraction of cholesterol from DHCR KO mast cells than from depleted or nondepleted WT cells (Fig. 3 C). These differences were significant and consistent with the in vitro experiments shown in Fig. 3 B.

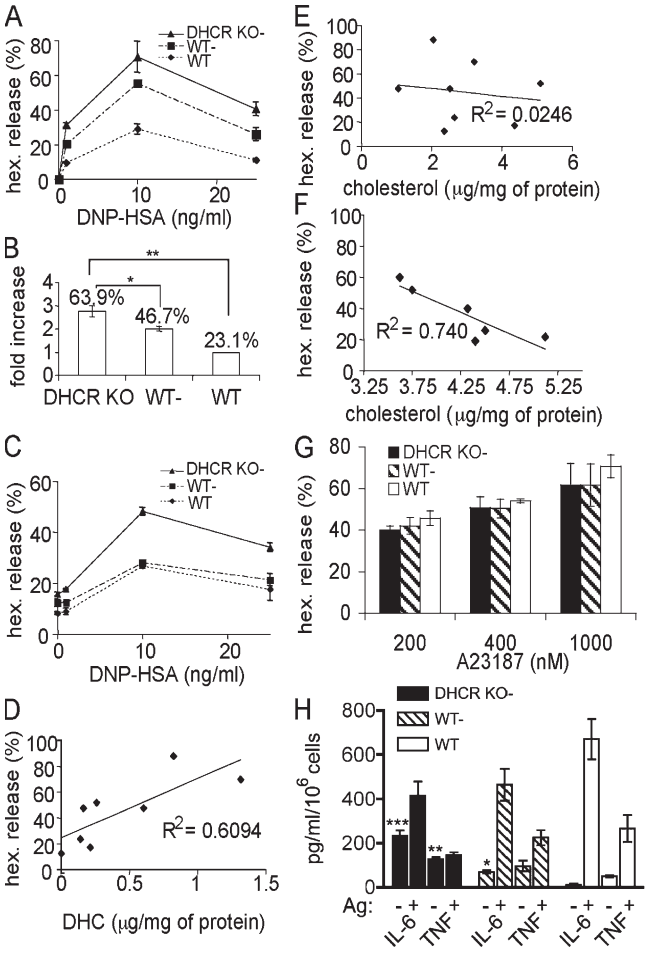

Figure 2. Cholesterol depletion and accumulation of DHC up-regulates mast cell degranulation and cytokine production. (A) WT and DHCR KO cells were cholesterol depleted (DHCR KO, WT-) or not (WT) for 72 h. The cells were sensitized with DNP-specific IgE for 60 min and activated by exposure to the indicated concentration of DNP-HSA for 20 min. Hexosaminidase release is expressed as a percentage of total cellular hexosaminidase. (B) Quantitative analysis of hexosaminidase release expressed as fold increase in cholesterol-depleted and nondepleted cells. The mean of hexosaminidase release calculated as in A from 15 experiments is shown above each genotype. *, $P < 0.02$; **, $P < 0.006$. (C) WT and DHCR KO cells were depleted as in A, sensitized with IgE, and cultivated for 30 min in media containing high levels of cholesterol. Hexosaminidase release (evaluated as in A) was compared with nondepleted WT mast cells. (D) Correlation of DHC with hexosaminidase release (*, $P < 0.02$) in DHCR KO cells. (E) Correlation of cholesterol with hexosaminidase release (*, $P > 0.70$) in DHCR KO cells. (F) Correlation of cholesterol with hexosaminidase release (*, $P < 0.01$) in WT cells. (G) Hexosaminidase release of cholesterol-depleted WT and DHCR KO mast cells and nondepleted WT mast cells treated with 20 ng/ml PMA and the indicated concentration of the calcium ionophore A23187. (H) IL-6 and TNF secretion in nondepleted (WT) and cholesterol-depleted (WT- and DHCR KO-) mast cells. Secreted cytokines were measured after cholesterol depletion from nonstimulated (−) or 10 ng/ml Ag-stimulated (+) cells. Data is the mean ± SEM from four individual experiments. *, $P < 0.05$; **, $P < 0.01$; ***, $P < 0.001$.

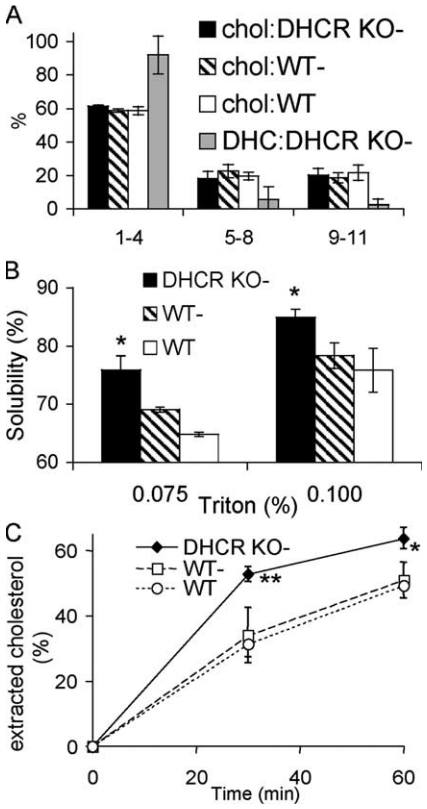

Figure 3. DHC reduces the stability of lipid rafts in mast cells. (A) Sterol analysis of sucrose density gradient fractions was performed by GC followed by mass spectrometry. Fractions 1–4 represent detergent-resistant membranes (lipid rafts). Amount of sterols is expressed as a percentage of the sterol found in the indicated pooled fractions compared with the total found in all fractions. (B) Solubility of multilamellar lipid vesicles prepared from cellular lipids was measured as a decrease of absorbance at 380 nm in 0.075 and 0.1% Triton X-100 at 30°C. Solubility is expressed as a percentage of the solubilized liposomes. *, $P < 0.01$ and < 0.03 for 0.075 and 0.1% Triton, respectively. (C) Cells were treated with 5 mM MBCD for the indicated time. The extracted cholesterol is reported as a percentage of the amount of cholesterol in MBCD-treated cells compared with the amount of cholesterol in nontreated cells. *, $P < 0.02$; **, $P < 0.003$. Data shown are from a minimum of three individual experiments.

Cholesterol depletion by MBCD can alter the localization of proteins associated with lipid rafts (13). We proposed that the cholesterol to DHC shift in cholesterol-depleted DHCR KO mast cells might cause or enhance alterations in protein localization. A substantial decrease in the previously described (4) lipid raft localization of FcεRI was observed in cholesterol-depleted DHCR KO mast cells (29.6 ± 4.1%) when compared with cholesterol-depleted (40.7 ± 2.4%) or nondepleted (43.4 ± 4.1%) WT mast cells (Fig. 4 A). These changes were not due to decreased FcεRI expression (Fig. 1 C) or to decreased recovery of soluble FcεRI as determined by bound radiolabeled IgE (WT/WT-/DHCR KO- = 1.0:1.02 ± 0.07:0.987 ± 0.09). A large fraction of Lyn kinase is also associated with lipid rafts in mast cells (14). This association may well depend on lipid raft stability given that the

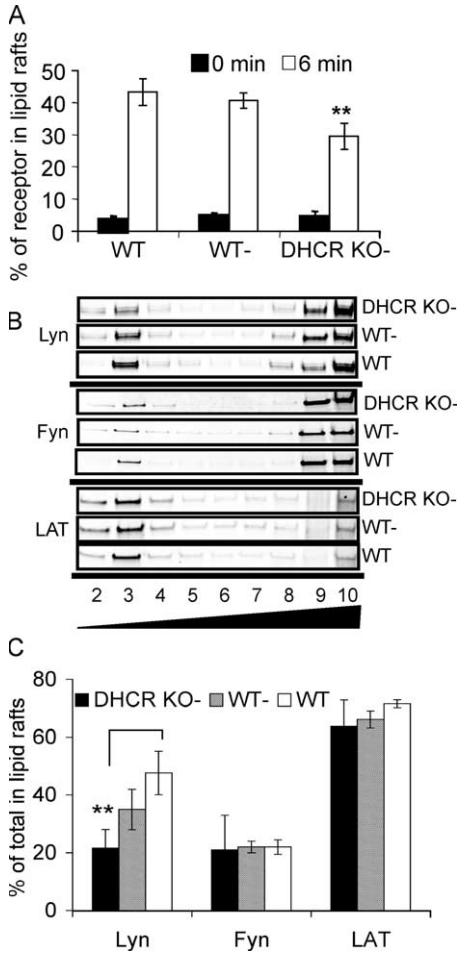

Figure 4. Reduced stability of lipid rafts in mast cells delocalizes select proteins. (A) Mast cells were labeled with [^{125}I]-IgE and activated with 100 ng/ml Ag for 6 min, and then solubilized in 0.1% Triton X-100. The percentage of FcεRI associated with detergent-resistant fractions (lipid rafts) was calculated from the lipid raft–associated cpm and the cpm in the entire gradient. **, $P < 0.001$ relative to WT. (B) Fractions of sucrose gradient that were analyzed are indicated along with increasing sucrose concentrations. Lyn, Fyn, and LAT were identified with specific antibodies. One representative of six experiments is shown. (C) Statistical analysis of Lyn, Fyn, and LAT association with lipid rafts (**, $P < 0.009$) for all experiments.

detectable fraction of Lyn within these domains can vary depending on the solubilization conditions (15). Solubilization of WT cells in 0.1% Triton X-100 showed that 51 ± 5% of total cellular Lyn was associated with lipid rafts (Fig. 4, B and C; $n = 6$). Depletion of cholesterol from WT cells decreased the amount of Lyn associated with lipid rafts to 36 ± 6%. Localization of Lyn to lipid rafts, however, was dramatically reduced (20 ± 8%, $P < 0.009$) when cholesterol was depleted from DHCR KO mast cells. Total recovery of cellular Lyn, as determined by densitometry of immunoblots, did not differ substantially (Fig. 5 A, WT/WT-/DHCR KO- = 1.0:0.923 ± 0.09:0.992 ± 0.14). Fyn kinase (~20 ± 5% of total) and the adaptor LAT (~80 ± 4% of total) also associate with lipid rafts in mast cells. However, neither cholesterol depletion nor DHC accumulation caused a substantial change in Fyn or LAT association with lipid rafts (Fig. 4, B and C). Quantitation of Fyn content in lipid rafts of cholesterol-depleted DHCR KO mast cells showed considerable variability; however, no considerable difference was found among the genotypes (percentage; WT, 22 ± 2.4; WT-, 22 ± 1.9; DHCR KO-, 21 ± 7.7; $n = 6$). Recovery of total cellular Fyn was similar among the genotypes (WT/WT-/DHCR KO- = 1.0:0.936 ± 0.11:0.947 ± 0.17). Collectively, the findings demonstrate that decreased lipid raft stability causes selective loss of some proteins (like Lyn kinase) from these domains, which might alter cellular signaling and responses.

Cholesterol depletion and DHC accumulation alter FcεRI–mediated early signaling upstream of calcium responses

The selective delocalization of Lyn kinase from lipid rafts in cholesterol-depleted DHCR KO mast cells led us to explore its cellular activity. To formally address the issue of the effect of Lyn displacement on its activity, we isolated Lyn from whole cell lysates as well as from the lipid raft fractions of nondepleted or cholesterol-depleted WT and DHCR KO mast cells. Fig. 5 A shows that the total Lyn kinase activity in cholesterol-depleted WT and DHCR KO mast cells did not differ substantially from that in nondepleted WT mast cells. In contrast, Lyn activity in lipid rafts was dramatically decreased upon cholesterol depletion of WT and DHCR KO mast cells relative to nondepleted WT mast cells (Fig. 5 B). The loss of Lyn activity in these domains led us to assess the phosphorylation of FcεRI in cholesterol-depleted DHCR KO cells. Fig. 5 C shows that the overall phosphorylation of FcεRI was decreased by cholesterol depletion. Densitometric quantitation demonstrated significant differences (*, $P < 0.05$; **, $P < 0.01$; $n = 4$). Although the kinetics were unaltered, the extent of FcεRIβ and FcεRIγ phosphorylation was reduced by ~30–40%.

Downstream of Lyn kinase, Syk kinase is activated by binding the ITAM sequences in the cytoplasmic domain of the γ subunit of FcεRI. Tyrosine (Y)346 in the linker region of Syk has been reported to be involved in the interaction and/or tyrosine phosphorylation and activation of phospholipase C-γ (PLCγ; reference 16). The linker region tyrosines are also possible targets of Lyn kinase activity (17). Phosphorylation of Syk Y346 in nondepleted WT mast cells was rapid (1 min) and increased sixfold after Ag stimulation (Fig. 5 D). In contrast, Syk Y346 phosphorylation in cholesterol-depleted WT and DHCR KO cells was delayed (>3 min) and reduced in magnitude (~50% inhibition). LAT, the adaptor that scaffolds a signaling complex that includes PLCγ, is a target of Syk activity (18). Because we previously showed that Y195 of LAT contributes to stable PLCγ binding (19), we used a phosphospecific antibody to assess its phosphorylation. As shown in Fig. 5 D, phosphorylation of LAT in nondepleted WT mast cells increased by eightfold after FcεRI stimulation with maximal phosphorylation at 3 min. Depletion of cholesterol significantly prolonged

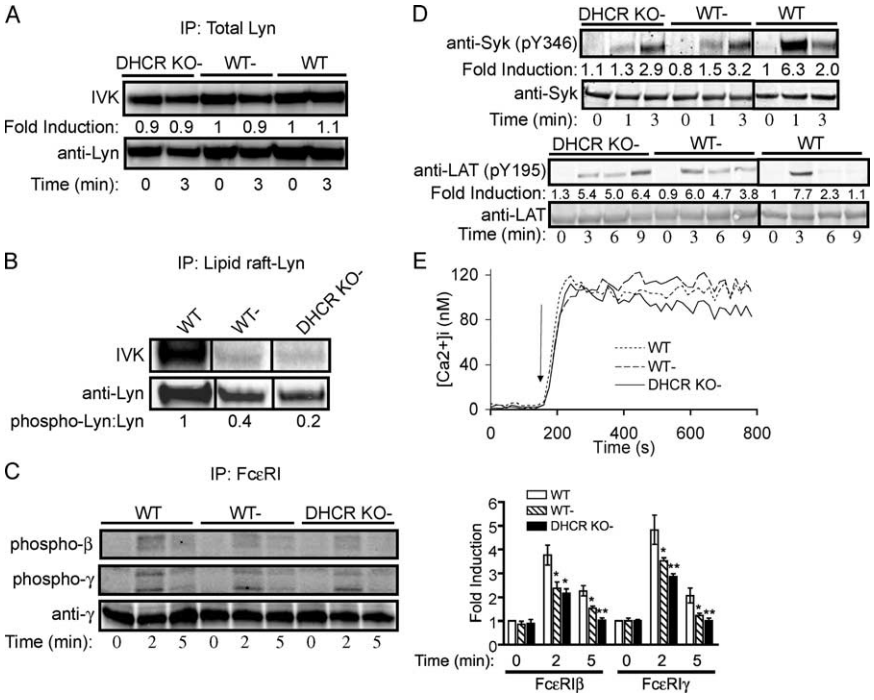

Figure 5. Reduced Lyn kinase activity and altered Syk, LAT, and FcεRI phosphorylation, but not calcium mobilization, in cholesterol-depleted WT and DHCR KO mast cells. In vitro kinase activity of immunoprecipitated Lyn (autophosphorylation) isolated from total cell lysates (A) or from the lipid raft fractions (B). For total and lipid raft–localized Lyn, activity is normalized to that activity in nondepleted WT cells. One representative of four individual experiments is shown. (C) Cholesterol-depleted WT and DHCR KO and nondepleted WT mast cells were activated with 100 ng Ag for the indicated time. IgE–FcεRI complexes were immunoprecipitated from the postnuclear supernatant using antibodies specific to IgE. Blots were probed with anti-phosphotyrosine–specific antibody 4G10 and anti-γ antibody. Fold increase is shown as a graph and was determined from three individual experiments. (D) Phosphorylation of Syk (Y346) and LAT (Y195) in cholesterol-depleted WT and DHCR KO mast cells as well as in nondepleted WT cells as detected with phosphospecific antibody. Fold induction reflects the increase in phosphoprotein/protein normalized to nonstimulated WT cells (1.0) in all panels. LAT (Y195) phosphorylation in cholesterol-depleted WT and DHCR KO mast cells as well as in nondepleted WT cells was detected with phosphospecific antibody. (E) Cholesterol-depleted WT and DHCR KO mast cells as well as nondepleted WT cells were loaded with Fura 2, and calcium mobilization was measured by fluorescence spectroscopy. Calcium mobilization is shown as the intracellular calcium concentration over time. Arrow indicates the addition of 20 ng Ag.

LAT Y195 phosphorylation for both WT and DHCR KO mast cells with peak responses reaching sixfold that of nonstimulated/nondepleted WT cells. Interestingly, DHCR KO mast cells showed a delay in maximal Y195 phosphorylation, demonstrating that the accumulation of DHC altered the kinetics. The sustained LAT phosphorylation suggested that PLCγ phosphorylation was unaltered, and no substantial differences were observed in the phosphorylation of PLCγ1 or PLCγ2 (not depicted). This was consistent with the small differences in the calcium response of nondepleted and cholesterol-depleted cells when normalized to the actual calcium concentration of each cell type after Fura 2 loading (Fig. 5 E). Thus, the findings demonstrate that the delocalization of a considerable fraction of Lyn protein after cholesterol depletion of DHCR KO mast cells reduced FcεRI phosphorylation, delayed Syk activation, and delayed LAT phosphorylation. However, the extent of LAT phosphorylation did not differ substantially from that of WT cells, consistent with no detectable alteration in PLCγ phosphorylation and calcium responses.

Cholesterol depletion enhances Fyn-mediated signaling; similarities with Lyn deficiency in mast cells

We and others previously demonstrated that the absence of Lyn in mast cells resulted in increased Fyn kinase activity and degranulation (20, 21). Failure to phosphorylate the Csk-binding protein (Cbp/PAG) and recruit the negative regulatory kinase, COOH-terminal Src kinase (Csk), was demonstrated as contributory to increased Fyn kinase activity (20). Because Cbp is present in lipid rafts, we speculated that Cbp phosphorylation might be impaired in cholesterol-depleted WT and DHCR KO mast cells. Phosphotyrosine analysis of immunoprecipitated Cbp demonstrated that cholesterol depletion of WT and DHCR KO mast cells resulted in decreased phosphorylation (Fig. 6 A). For cholesterol-depleted DHCR KO mast cells, the extent of phosphorylation was more appreciably reduced (greater than twofold difference relative to cholesterol-depleted WT cells). The activity of Fyn was increased three- to fivefold in cholesterol-depleted WT and DHCR KO mast cells relative to the nondepleted WT mast cells (Fig. 6 B).

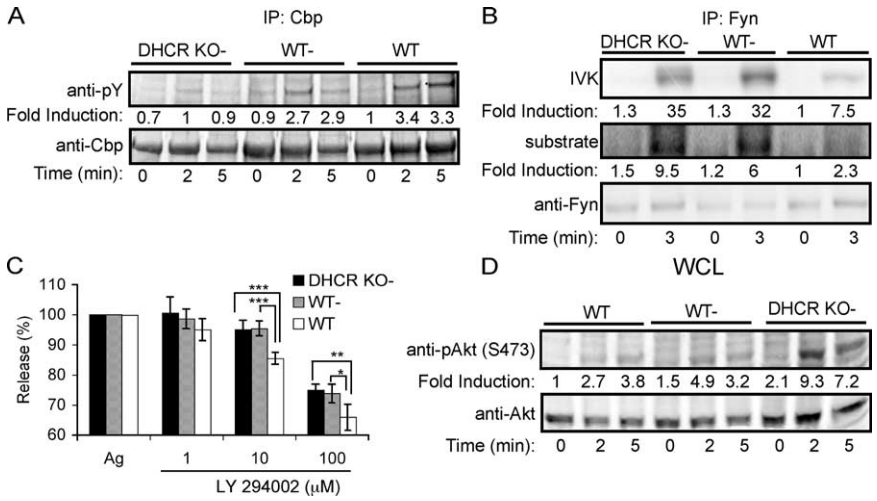

Figure 6. Up-regulation of Fyn kinase activity as a consequence of cholesterol depletion and DHC accumulation. (A) Cbp from cholesterol-depleted WT and DHCR KO mast cells as well as from nondepleted WT mast cells was immunoprecipitated with goat antibody to Cbp and probed with anti-phospho tyrosine and rabbit antibody to Cbp. Fold induction reflects the increase in phospho-protein/protein normalized to nonstimulated WT cells (1.0) in all panels. (B) In vitro kinase activity of Fyn before and after activation. Fyn kinase was immunoprecipitated from cell lysates and incubated in the presence of [^{32}P]-labeled ATP and dephosphorylated casein as a substrate for 20 min at 30°C. Both autophosphorylation and substrate phosphorylation are shown. (C) Mast cells were treated or not with the indicated concentrations of LY294002 and activated with 10 ng DNP-HSA, and hexosaminidase release was measured in three individual experiments. Release (%) is normalized to Ag-stimulated cells (100%) in the absence of LY294002. ***, $P < 0.001$; **, $P < 0.01$. Spontaneous release (~4%) did not differ in the presence or absence of the inhibitor. (D) Activation of Akt in cholesterol-depleted WT and DHCR KO mast cells as well as nondepleted WT mast cells. Phosphorylation was analyzed by probing of cell lysates after activation with 100 ng Ag using phosphospecific antibody to S473 of Akt. Fold increase in phosphorylation for all experiments is from a minimum of three individual experiments normalized to protein.

Our previous studies established that Fyn kinase is able to regulate the phosphorylation of Gab2 (22), an adaptor molecule demonstrated by others to directly modulate the activity of phosphatidylinositol 3-OH kinase (PI3K) and found to be essential for mast cell degranulation (23). To determine whether enhanced PI3K activity played a role in the enhanced degranulation phenotype observed upon cholesterol depletion, we treated cholesterol-depleted DHCR KO and WT cells with the PI3K-specific inhibitor, LY 294002. Cholesterol depletion of DHCR KO and WT mast cells caused increased resistance to this inhibitor (Fig. 6 C). At the suboptimal concentration of 10 μM, the degranulation of nondepleted WT mast cells was inhibited by 15.2 ± 2.1%, whereas degranulation of cholesterol-depleted WT and DHCR KO mast cells was inhibited by 5.1 ± 2.1% and 5.9 ± 1.8% ($P < 0.001$, $n = 3$), respectively. To further verify increased PI3K activity, we measured the phosphorylation of Akt, a kinase whose activity is dependent on PI3K-generated PIP_3. Phosphorylation of S473 of Akt in FcεRI-stimulated cholesterol-depleted DHCR KO cells was increased almost threefold compared with nondepleted WT and twofold relative to cholesterol-depleted WT mast cells (Fig. 6 D). Importantly, cholesterol depletion led to a twofold increase in constitutive phosphorylation of Akt in DHCR KO mast cells. This increase in Akt phosphorylation was consistent with our prior findings of increased constitutive S473 phosphorylation in Lyn-null bone marrow–derived mast cells (22).

DISCUSSION

Herein, we describe a genetic model in which mutation of the 3β-hydroxysterol Δ^7-reductase gene caused reduction of cholesterol in the absence of an exogenous agent. This SLOS model provides the first in vivo evidence in a genetic model that DHC can partition to lipid raft domains and cause lipid raft dysfunction. Previous findings, using artificial membranes or pharmacological inhibitors of 3β-hydroxysterol Δ^7-reductase, demonstrated that DHC is able to incorporate into lipid rafts and partitions more effectively than cholesterol (24). We now find that DHC is able to maintain the structural integrity of lipid rafts, albeit with clear differences in domain stability and cell signaling. In contrast, desmosterol (the sterol accumulating in cholesterol-depleted WT cells) partitions poorly to lipid rafts but has been demonstrated to partly alter cell signaling (25). However, accumulation of desmosterol in cells was more variable and together with the reduced levels of cholesterol in WT cells (at 72 h of depletion) could provide an explanation for the milder and more variable phenotype (degranulation, cytokine production, lipid raft instability, and Lyn displacement) of the cholesterol-depleted WT mast cells. Regardless, the reversal of the hyper-degranulation in cholesterol-depleted WT cells by repletion of cholesterol demonstrated that this sterol principally accounts for the alteration of degranulation observed for WT cells. This is consistent with the prior finding that acute lowering of cholesterol enhances mast cell degranulation (26). The implication is that altered localization of signaling proteins, as a consequence of

either cholesterol deficiency and/or DHC accumulation, contributes to the SLOS phenotype.

Several studies promote the view that cholesterol is key in compartmentalizing signaling during growth, differentiation, and function. In the immune system, tolerance-sensitive transitional immature B cells with low levels of cholesterol showed impaired localization of the B cell Ag receptor in lipid rafts after engagement of this receptor, as well as altered signaling (27). In embryonic development, Hedgehog signaling requires cholesterol for its appropriate function. Sonic, Indian, and Desert Hedgehogs, which are involved in limb and midline pattern formation, bone mineralization, and genital development, respectively, are covalently modified by the addition of cholesterol to their amino-terminal signaling domain, which is required for their appropriate function (28, 29). The work of Drs. Baird and Holowka has provided ample evidence of a key role for cholesterol-enriched lipid rafts in FcεRI phosphorylation and mast cell activation. The evidence is multifaceted: (a) the fraction of FcεRI found in cholesterol-rich membranes is rapidly increased upon receptor engagement, and these regions also contain a large fraction of Lyn kinase (4, 14); (b) the active fraction of Lyn kinase is primarily found in cholesterol-rich membranes, and this environment protects included proteins from dephosphorylation by phosphatases (30); (c) a large proportion of phosphorylated FcεRI is also found within these domains relative to that outside of these regions (5); and (d) depletion of cholesterol by pharmacological agents caused reduced phosphorylation of FcεRI (5). However, considerable evidence to the contrary also exists. Collectively, this apparently contradictory evidence suggests that the presence of FcεRI or Lyn in lipid rafts is not essential for FcεRI phosphorylation (10, 15, 31, 32). We now demonstrate that phosphorylation of FcεRI is altered by cholesterol depletion, arguing in favor of a role for lipid raft–localized Lyn in this event. However, the kinetics of FcεRI phosphorylation were unaltered, suggesting that Lyn outside of lipid rafts may also contribute to receptor phosphorylation. This latter view is also supported by the fact that with 80% of Lyn activity lost from lipid rafts of cholesterol-depleted DHCR KO mast cells, the inhibition of receptor phosphorylation was at best 40%. Recent studies also demonstrate that mutation of the FcεRIβ ITAM, which ablates the interaction of Lyn with receptor, inhibited the initiation of FcεRI phosphorylation (33, 34), arguing that protein–protein interaction of Lyn with FcεRI is required for either initiation or sustaining phosphorylation. Thus, a cohesive model is one in which protein interaction of FcεRI with Lyn is important for the initiation of receptor phosphorylation, whereas the cholesterol-enriched environment, which includes a significant fraction of Lyn, may function to amplify this interaction and sustain receptor phosphorylation. This model incorporates the protective phosphatase-deficient environment of lipid raft domains (30) as important in maintaining the phosphorylated state of the receptor.

The work described herein also argues that Lyn kinase has functions outside as well as inside lipid raft domains. For example, one might attribute Cbp phosphorylation as a lipid raft localized function of Lyn because Cbp is lipid raft localized and Lyn-null mast cells were equally defective in Cbp phosphorylation (20). The phosphorylation of FcεRI and Syk, however, is seemingly a function of Lyn both inside and outside of lipid rafts. Syk activation, which depends on FcεRI phosphorylation, peaked at ~50–60% of that in nondepleted WT cells (as measured by phosphorylation) but still caused sustained LAT phosphorylation and thus normal PLCγ phosphorylation and calcium responses. In contrast, Lyn-null mast cells showed a marked defect in calcium responses (22, 35, 36), which is consistent with a more appreciable defect in Syk and LAT phosphorylation.

Although the phenotype of cholesterol depletion in WT and DHCR KO mast cells is not entirely consistent with Lyn-null mast cells, significant similarities exist. Increased activity of Fyn in DHCR KO cells, relative to cholesterol-depleted WT cells, was consistent with Lyn-null mast cells. Loss of Cbp phosphorylation was demonstrated to cause increased Fyn activity in Lyn-null bone marrow–derived mast cell (20). Now we find that cholesterol-depleted DHCR KO mast cells showed a pronounced loss of Cbp phosphorylation relative to that seen in cholesterol-depleted or nondepleted WT mast cells. This would indicate that the DHC-mediated maintenance of a hyperresponsive mast cell is, at least in part, dependent on the loss of Cbp phosphorylation causing increased Fyn kinase activity. It is notable that Fyn kinase activity was also increased in cholesterol-depleted WT mast cells in conjunction with a reduction in Cbp phosphorylation. The increased Fyn activity and constitutive activation of Akt in both cholesterol-depleted WT and DHCR KO mast cells are also consistent with the constitutive secretion of cytokines. Our recent study (37) demonstrates that Fyn is required for cytokine production and deficiency in Fyn kinase results in reduced Akt phosphorylation and nuclear NFκB activity, an activity required for both IL-6 and TNF production. Although the constitutive activity of Fyn upon cholesterol depletion of WT and DHCR KO mast cells was modest (WT/WT-/DHCR KO- = 1.0:1.2 ± 0.04:1.5 ± 0.06; $P < 0.05$, $n = 3$), it was significant and sustained. Thus, the constitutive signaling in the absence of cholesterol could drive the cytokine production observed and contribute to the sensitivity of SLOS patients to allergic inflammation.

Clinical treatment of SLOS patients includes placing these patients on a cholesterol-rich diet, which allows better management of the multiple aberrant behavioral characteristics and enhances patient quality of life, but does little to alter the fixed developmental abnormalities (38). Reports of allergies for these patients are for the most part anecdotal, but an increase in diet cholesterol allows better food tolerance and may decrease the frequency of other allergic-like and inflammatory manifestations. Unlike for WT mast cells, cholesterol repletion of DHCR KO mast cells did not completely reverse the hyper-degranulation. This suggests that SLOS patients possess and maintain (even in the presence of a cholesterol-rich diet) lipid raft dysfunctions and increased mast cell

sensitivity relative to normal individuals. This is consistent with the continued accumulation of DHC in patients on a cholesterol-rich diet. Thus, one might speculate that a weak allergic stimulus may be sufficient to elicit unwanted mast cell responses in SLOS. This does not appear to be mediated through increased total IgE production, as our initial screening of patient serum did not reveal abnormal levels (not depicted). Whether increased allergen-specific IgE occurs in these patients remains to be determined. Regardless, the findings point to a dysregulation of lipid raft function and cell signaling as a possible underlying cause of some of the developmental and neurological problems in SLOS. The observation of lipid raft dysregulation due to DHC strongly supports the use of a therapeutic strategy designed to lower DHC levels in addition to cholesterol supplementation.

MATERIALS AND METHODS

Antibodies and reagents. mAbs to Syk (clone 4D10), phosphotyrosine (clone 4G10), and polyclonal anti-pY191 LAT were from Upstate Biotechnology. Rabbit polyclonal antibody to Lyn, Fyn, and goat anti-Cbp (P-18) were from Santa Cruz Biotechnology, Inc. Phosphospecific antibodies to Syk, Akt, and ERK, as well as mAbs Akt and ERK were from Cell Signaling Technology. Rabbit polyclonal anti-Cbp and mouse mAbs anti-LAT were provided by T. Yamashita (Hokkaido University, Sapporo, Japan) and P. Draber (Institute of Molecular Genetics, Prague, Czech Republic), respectively. Chicken anti-Fyn antibody was prepared by Aves Labs, Inc. using peptide sequence CKDKEAAKLTEERDGSLNQS from the unique domain of Fyn. FITC-conjugated monoclonal rat anti–mouse IgE and FITC-conjugated rat IgG1 monoclonal Ig isotype standard (both used in flow cytometry) were from BD Biosciences. Cy5.5-conjugated anti–chicken, avidin, and anti–rabbit antibody, as well as IRDye800-conjugated anti–mouse were from Rockland, Inc. Mouse DNP–specific IgE was produced as described previously (39). Cell culture media (EMEM, DMEM, and RPMI 1640) was prepared as described previously (22, 40). β-octyl-glucoside was from Pierce Chemical Co., [^{32}P]-ATP was from AP Biomedical, and FURA 2 was from Invitrogen. Other described reagents were from Sigma-Aldrich.

Cell culture, cell stimulation, degranulation, and cytokine assays. Mast cells were cultured from liver progenitors. Cells from the livers of newborn mice were isolated using a cell strainer (40 μm; Falcon; BD Biosciences), washed in RPMI media twice, and cultured as described previously (40) in the presence of 20 ng/ml IL-3 and 20 ng/ml stem cell factor. Mast cell populations were monitored for c-KIT and FcεRI expression by flow cytometric analysis (41). Mature mast cells were sensitized with anti-DNP mouse IgE (1 μg per 10^7 cells) for 2 h in culture medium, and then washed twice with Tyrode-BSA buffer (22, 40). Cell aliquots of 3×10^7 were resuspended in a total volume of 4 ml Tyrode buffer, stimulated with the indicated Ag concentrations, and sampled at the indicated times.

Degranulation was determined by a colorimetric assay measuring β-hexosaminidase activity in a 96-well format essentially as described previously (40). Cytokine secretion was measured by ELISA (R&D Systems) as described previously (37).

Cell lysates, immunoprecipitation, and immunoblotting. Cell lysates were prepared in borate buffer as described previously (42) with the exception of lysates for immunoprecipitation and analysis of Fyn activity, which were solubilized in RIPA buffer (10 mM NaH_2PO_4, 50 mM NaCl, 50 mM NaF, 0.5% sodium deoxycholate, 0.05% NaN_3, 0.1% SDS, 1% Triton, 1 mM Na_3VO_4). Cell lysates were precleared with protein A or protein G sepharose beads for 1 h and incubated for 2 h with antibodies prebound to either protein G sepharose (goat polyclonal) or protein A sepharose (rabbit polyclonal). Beads were washed three times, and proteins were recovered with 30 μl of 2× concentrated Tris-glycine SDS sample buffer that contained 1% 2-ME and 1 mM Na_3VO_4. For immunoblotting, proteins were resolved by 8, 10, or 12% SDS-PAGE (Invitrogen) and electrophoretically transferred to nitrocellulose membranes (Invitrogen or Schleicher and Schuell). Nitrocellulose membranes were blocked with Odyssey blocking buffer (LI-COR Biosciences). They were then probed with the desired primary antibody in blocking buffer containing 0.1% Tween-20, and then with an appropriate Cy5.5 and/or IRDye800-conjugated secondary antibody and visualized by Odyssey Infrared Imaging System (LI-COR Biosciences).

Cholesterol depletion, sterol analysis of cell pellets, preparation and solubilization of multilamellar vesicles, and isolation of lipid rafts. For cholesterol depletion, cells were incubated in cholesterol-free medium with 10% LPDS. LPDS was prepared by organic extraction of FBS in a mixture of *n*-butanol and isopropylether (5:4:6) for 1 h in the dark and centrifuged for 15 min at 4,000 *g*. The bottom phase was recovered and lyophilized, and the resulting pellet was resuspended in original volume. Cholesterol content of LPDS was determined by GC/mass spectrometry and found to be 130 ± 28 pg/ml (normal levels are 10–20 ng/ml). For sterol analysis, cell pellets were frozen and thawed twice. After saponification and lipid extraction, the cell sterols were subjected to GC/mass spectrometry as described previously (43). Protein content of the samples was determined by BCA protein assay (Pierce Chemical Co.).

Preparation of multilamellar vesicles was accomplished by extraction of lipids from 10^7 cells with 25 mM HCl methanol/chloroform/1M NaCl (1:1:1). The organic phase was assayed for total phospholipid content as described previously (44). 500 nmol of total phospholipids from the organic phase of each sample was dried under N_2 for 20 min. The resulting pellet was resuspended in 1 ml PBS with three strokes of ultrasound probe (12% amplification). Vesicle solubility experiments used 200 μl of multilamellar vesicles in a 96-well plate (Immulon 1B). Solubility was achieved by adding 5 μl of 1% Triton X-100 (10-min intervals) and measuring a decrease in absorbance (at 20-s intervals) at 380 and 450 nm on a Fluostar Optima spectrometer (BMG Labtechnologies). Solubility of multilamellar vesicles in Triton X-100 was calculated from the average absorbance at 5 min after the addition of detergent and expressed as the percentage of solubilized liposomes relative to total unsolubilized liposomes.

Lipid rafts were isolated as described previously (15) with some modifications. In brief, Ag-stimulated (100 ng/ml, 3 min) cells (4.0×10^7) or non-stimulated cells were lysed in 1 ml of cold 0.1% Triton X-100, which contained protease inhibitors, and were homogenized by passing the cells through a 25-gauge needle. Homogenates were loaded directly on sucrose gradients without preclearing. Gradient fractions were collected from the top of the gradient (low to high density), and fractions 1 and 2 or 10 and 11 were pooled. All other fractions were kept individually. For isolation of Lyn from lipid rafts, fractions 1–5 were pooled resuspended in 2× RIPA buffer and Lyn was immunoprecipitated as describe above.

In vitro kinase assay and calcium measurements. The activity of Lyn or Fyn kinase was measured by an immune complex in vitro kinase assay. 3.0×10^7 mast cells were lysed in RIPA buffer as described above. Lyn and Fyn were immunoprecipitated with 5 μg of the appropriate antibody prebound to protein A sepharose beads for 3 h at 4°C. Immune-complexed proteins were recovered by centrifugation and washed twice with RIPA buffer followed by two additional washes with kinase buffer (50 mM Hepes, 0.1 mM EDTA, 0.015% Triton X-100, 0.07% 2-ME, 10 μM Na3VO4, pH 7.0). The in vitro kinase reaction was started by resuspension of the recovered pellet in 30 μl of kinase buffer containing 10 mM ATP, 1 μCi [^{32}P]-labeled ATP, and 10 mM $MgCl_2$. 10 μg dephosphorylated casein was added as an exogenous substrate. Samples were incubated at 30°C for 20 min with vigorous mixing, and reactions were stopped by the addition of 30 μl 2× SDS sample buffer and immediate boiling for 3 min. Protein A sepharose beads were removed by centrifugation, and recovered proteins were resolved by SDS-PAGE and transferred to nitrocellulose membranes. Autophosphorylation of each kinase or phosphorylation of exogenous substrate was detected by phosphoimager after transfer of proteins to nitrocellulose membranes.

Protein loading was determined by probing the membranes with appropriate antibodies, and quantification was performed by densitometry.

For calcium measurements, 2×10^6 cells were loaded with IgE (1 μg/10^7 cells) and 2 μM FURA-2/AM (Invitrogen) in RPMI 2% FBS media for 45 min at 37°C. Cells were washed twice in Tyrodes-BSA, and changes in dye fluorescence with time were determined by Fluostar Optima spectrometer (BMG Labtechnologies) with excitation wavelengths of 340 and 380 nm and with a constant emission at 510 nm. Calcium concentrations were calculated as described previously (45).

Online supplemental material. Fig. S1, which shows the kinetics of proliferation of nondepleted WT and cholesterol-depleted WT and DHCR KO mast cells, is available at http://www.jem.org/cgi/content/full/jem.20051701/DC1.

This research was supported by the Intramural Research Program of the NIH, National Institute of Arthritis and Musculoskeletal and Skin Diseases, and National Institute of Child Health and Human Development. Additional support was provided by the United States-Israel Binational Science Foundation (to J. Rivera, grant no. 2000016).

The authors have no conflicting financial interests.

Submitted: 23 August 2005
Accepted: 22 March 2006

REFERENCES

1. Wassif, C.A., C. Maslen, S. Kachilele-Linjewile, D. Lin, L.M. Linck, W.E. Connor, R.D. Steiner, and F.D. Porter. 1998. Mutations in the human sterol Δ7-reductase gene at 11q12-13 cause Smith-Lemli-Opitz syndrome. *Am. J. Hum. Genet.* 63:55–62.
2. Waterham, H.R., F.A. Wijburg, R.C. Hennekam, P. Vreken, B.T. Poll-The, L. Dorland, M. Duran, P.E. Jira, J.A. Smeitink, R.A. Wevers, and R.J. Wanders. 1998. Smith-Lemli-Opitz syndrome is caused by mutations in the 7-dehydrocholesterol reductase gene. *Am. J. Hum. Genet.* 63:329–338.
3. Fitzky, B.U., M. Witsch-Baumgartner, M. Erdel, J.N. Lee, Y.K. Paik, H. Glossmann, G. Utermann, and F.F. Moebius. 1998. Mutations in the Δ7-sterol reductase gene in patients with the Smith-Lemli-Opitz syndrome. *Proc. Natl. Acad. Sci. USA.* 95:8181–8186.
4. Field, K.A., D. Holowka, and B. Baird. 1997. Compartmentalized activation of the high affinity immunoglobulin E receptor within membrane domains. *J. Biol. Chem.* 272:4276–4280.
5. Sheets, E.D., D. Holowka, and B. Baird. 1999. Critical role for cholesterol in Lyn-mediated tyrosine phosphorylation of FcεRI and their association with detergent-resistant membranes. *J. Cell Biol.* 145:877–887.
6. Wassif, C.A., P. Zhu, L. Kratz, P.A. Krakowiak, K.P. Battaile, F.F. Weight, A. Grinberg, R.D. Steiner, N.A. Nwokoro, R.I. Kelley, et al. 2001. Biochemical, phenotypic and neurophysiological characterization of a genetic mouse model of RSH/Smith-Lemli-Opitz syndrome. *Hum. Mol. Genet.* 10:555–564.
7. Brown, D.A., and E. London. 2000. Structure and function of sphingolipid- and cholesterol-rich membrane rafts. *J. Biol. Chem.* 275: 17221–17224.
8. Simons, K., and D. Toomre. 2000. Lipid rafts and signal transduction. *Nat. Rev. Mol. Cell Biol.* 1:31–39.
9. London, E., and D.A. Brown. 2000. Insolubility of lipids in triton X-100: physical origin and relationship to sphingolipid/cholesterol membrane domains (rafts). *Biochim. Biophys. Acta.* 1508:182–195.
10. Vonakis, B.M., H. Chen, H. Haleem-Smith, and H. Metzger. 1997. The unique domain as the site on Lyn kinase for its constitutive association with the high affinity receptor for IgE. *J. Biol. Chem.* 272:24072–24080.
11. Xu, X., R. Bittman, G. Duportail, D. Heissler, C. Vilcheze, and E. London. 2001. Effect of the structure of natural sterols and sphingolipids on the formation of ordered sphingolipid/sterol domains (rafts). Comparison of cholesterol to plant, fungal, and disease-associated sterols and comparison of sphingomyelin, cerebrosides, and ceramide. *J. Biol. Chem.* 276:33540–33546.
12. Ramstedt, B., and J.P. Slotte. 1999. Comparison of the biophysical properties of racemic and d-erythro-N-acyl sphingomyelins. *Biophys. J.* 77:1498–1506.
13. Horejsi, V. 2002. Membrane rafts in immunoreceptor signaling: new doubts, new proofs? *Trends Immunol.* 23:562–564.
14. Field, K.A., D. Holowka, and B. Baird. 1995. FcεRI-mediated recruitment of p53/56lyn to detergent-resistant membrane domains accompanies cellular signaling. *Proc. Natl. Acad. Sci. USA.* 92:9201–9205.
15. Kovarova, M., P. Tolar, R. Arudchandran, L. Draberova, J. Rivera, and P. Draber. 2001. Structure-function analysis of Lyn kinase association with lipid rafts and initiation of early signaling events after Fcε receptor I aggregation. *Mol. Cell. Biol.* 21:8318–8328.
16. Law, C.L., K.A. Chandran, S.P. Sidorenko, and E.A. Clark. 1996. Phospholipase C-γ1 interacts with conserved phosphotyrosyl residues in the linker region of Syk and is a substrate for Syk. *Mol. Cell. Biol.* 16:1305–1315.
17. Keshvara, L.M., C.C. Isaacson, T.M. Yankee, R. Sarac, M.L. Harrison, and R.L. Geahlen. 1998. Syk- and Lyn-dependent phosphorylation of Syk on multiple tyrosines following B cell activation includes a site that negatively regulates signaling. *J. Immunol.* 161:5276–5283.
18. Rivera, J. 2002. Molecular adapters in FcεRI signaling and the allergic response. *Curr. Opin. Immunol.* 14:688–693.
19. Saitoh, S., S. Odom, G. Gomez, C.L. Sommers, H.A. Young, J. Rivera, and L.E. Samelson. 2003. The four distal tyrosines are required for LAT-dependent signaling in FcεRI-mediated mast cell activation. *J. Exp. Med.* 198:831–843.
20. Odom, S., G. Gomez, M. Kovarova, Y. Furumoto, J.J. Ryan, H.V. Wright, C. Gonzalez-Espinosa, M.L. Hibbs, K.W. Harder, and J. Rivera. 2004. Negative regulation of immunoglobulin E–dependent allergic responses by Lyn kinase. *J. Exp. Med.* 199:1491–1502.
21. Hernandez-Hansen, V., A.J. Smith, Z. Surviladze, A. Chigaev, T. Mazel, J. Kalesnikoff, C.A. Lowell, G. Krystal, L.A. Sklar, B.S. Wilson, and J.M. Oliver. 2004. Dysregulated FcεRI signaling and altered Fyn and SHIP activities in Lyn-deficient mast cells. *J. Immunol.* 173:100–112.
22. Parravicini, V., M. Gadina, M. Kovarova, S. Odom, C. Gonzalez-Espinosa, Y. Furumoto, S. Saitoh, L.E. Samelson, J.J. O'Shea, and J. Rivera. 2002. Fyn kinase initiates complementary signals required for IgE-dependent mast cell degranulation. *Nat. Immunol.* 3:741–748.
23. Gu, H., K. Saito, L.D. Klaman, J. Shen, T. Fleming, Y. Wang, J.C. Pratt, G. Lin, B. Lim, J.P. Kinet, and B.G. Neel. 2001. Essential role for Gab2 in the allergic response. *Nature.* 412:186–190.
24. Keller, R.K., T.P. Arnold, and S.J. Fliesler. 2004. Formation of 7-dehydrocholesterol-containing membrane rafts in vitro and in vivo, with relevance to the Smith-Lemli-Opitz syndrome. *J. Lipid Res.* 45:347–355.
25. Vainio, S., M. Jansen, M. Koivusalo, T. Rog, M. Karttunen, I. Vattulainen, and E. Ikonen. 2006. Significance of sterol structural specificity. Desmosterol cannot replace cholesterol in lipid rafts. *J. Biol. Chem.* 281:348–355.
26. Surviladze, Z., L. Draberova, M. Kovarova, M. Boubelik, and P. Draber. 2001. Differential sensitivity to acute cholesterol lowering of activation mediated via the high-affinity IgE receptor and Thy-1 glycoprotein. *Eur. J. Immunol.* 31:1–10.
27. Karnell, F.G., R.J. Brezski, L.B. King, M.A. Silverman, and J.G. Monroe. 2005. Membrane cholesterol content accounts for developmental differences in surface B cell receptor compartmentalization and signaling. *J. Biol. Chem.* 280:25621–25628.
28. Cohen, M.M., Jr. 2003. The hedgehog signaling network. *Am. J. Med. Genet. A.* 123:5–28.
29. Nybakken, K., and N. Perrimon. 2002. Hedgehog signal transduction: recent findings. *Curr. Opin. Genet. Dev.* 12:503–511.
30. Young, R.M., D. Holowka, and B. Baird. 2003. A lipid raft environment enhances Lyn kinase activity by protecting the active site tyrosine from dephosphorylation. *J. Biol. Chem.* 278:20746–20752.
31. Vonakis, B.M., H. Haleem-Smith, P. Benjamin, and H. Metzger. 2001. Interaction between the unphosphorylated receptor with high affinity for IgE and Lyn kinase. *J. Biol. Chem.* 276:1041–1050.
32. Wofsy, C., B.M. Vonakis, H. Metzger, and B. Goldstein. 1999. One lyn molecule is sufficient to initiate phosphorylation of aggregated high-affinity IgE receptors. *Proc. Natl. Acad. Sci. USA.* 96:8615–8620.

33. Furumoto, Y., S. Nunomura, T. Terada, J. Rivera, and C. Ra. 2004. The FcεRIβ immunoreceptor tyrosine-based activation motif exerts inhibitory control on MAPK and IκB kinase phosphorylation and mast cell cytokine production. *J. Biol. Chem.* 279:49177–49187.
34. On, M., J.M. Billingsley, M.H. Jouvin, and J.P. Kinet. 2004. Molecular dissection of the FcRβ signaling amplifier. *J. Biol. Chem.* 279:45782–45790.
35. Nishizumi, H., and T. Yamamoto. 1997. Impaired tyrosine phosphorylation and Ca2+ mobilization, but not degranulation, in Lyn-deficient bone marrow-derived mast cells. *J. Immunol.* 158:2350–2355.
36. Kawakami, Y., J. Kitaura, A.B. Satterthwaite, R.M. Kato, K. Asai, S.E. Hartman, M. Maeda-Yamamoto, C.A. Lowell, D.J. Rawlings, O.N. Witte, and T. Kawakami. 2000. Redundant and opposing functions of two tyrosine kinases, Btk and Lyn, in mast cell activation. *J. Immunol.* 165:1210–1219.
37. Gomez, G., C. Gonzalez-Espinosa, S. Odom, G. Baez, M.E. Cid, J.J. Ryan, and J. Rivera. 2005. Impaired FcεRI-dependent gene expression and defective eicosanoid and cytokine production as a consequence of Fyn-deficiency in mast cells. *J. Immunol.* 175:7602–7610.
38. Porter, F.D. 2003. Human malformation syndromes due to inborn errors of cholesterol synthesis. *Curr. Opin. Pediatr.* 15:607–613.
39. Liu, F.T., J.W. Bohn, E.L. Ferry, H. Yamamoto, C.A. Molinaro, L.A. Sherman, N.R. Klinman, and D.H. Katz. 1980. Monoclonal dinitrophenyl-specific murine IgE antibody: preparation, isolation, and characterization. *J. Immunol.* 124:2728–2737.
40. Saitoh, S., R. Arudchandran, T.S. Manetz, W. Zhang, C.L. Sommers, P.E. Love, J. Rivera, and L.E. Samelson. 2000. LAT is essential for FcεRI-mediated mast cell activation. *Immunity.* 12:525–535.
41. Manetz, T.S., C. Gonzalez-Espinosa, R. Arudchandran, S. Xirasagar, V. Tybulewicz, and J. Rivera. 2001. Vav1 regulates phospholipase Cγ activation and calcium responses in mast cells. *Mol. Cell. Biol.* 21: 3763–3774.
42. Arudchandran, R., M.J. Brown, M.J. Peirce, J.S. Song, J. Zhang, R.P. Siraganian, U. Blank, and J. Rivera. 2000. The Src homology 2 domain of Vav is required for its compartmentation to the plasma membrane and activation of c-jun NH(2)-terminal kinase 1. *J. Exp. Med.* 191:47–60.
43. Wassif, C.A., P.A. Krakowiak, B.S. Wright, J.S. Gewandter, A.L. Sterner, N. Javitt, A.L. Yergey, and F.D. Porter. 2005. Residual cholesterol synthesis and simvastatin induction of cholesterol synthesis in Smith-Lemli-Opitz syndrome fibroblasts. *Mol. Genet. Metab.* 85: 96–107.
44. Edsall, L.C., and S. Spiegel. 1999. Enzymatic measurement of sphingosine 1-phosphate. *Anal. Biochem.* 272:80–86.
45. Petr, M.J., and R.D. Wurster. 1997. Determination of in situ dissociation constant for Fura-2 and quantitation of background fluorescence in astrocyte cell line U373-MG. *Cell Calcium.* 21:233–240.